===== **COMPOSITES** =====

PTMG-Modified MWCNT/PTMG-Based Polyurethane Nanocomposites: Strong Interaction and Homogeneous Dispersion[1]

Hossein Behniafar* and Mojtaba Yazdi

Faculty of Chemistry, Damghan University, Damghan, 36715-364 Iran

*e-mail: h_behniafar@du.ac.ir

Abstract—Soft and flexible chains of poly(tetramethylene glycol) (PTMG) were covalently grafted with multi-walled carbon nanotubes (MWCNT). FE-SEM images showed that the polyether PTMG formed a surrounding shell around the nanotubes with about 5 nm in thickness. The modified nanotubes (MWCNT-PTMG) were then loaded into an in situ prepared polyurethane elastomer (PUE) with different loading contents below 1 wt %. In addition to the modifier of MWCNT, polyether PTMG was also used for preparing the polyurethane matrix. Thermal analyses (TG/DTG and DTA) showed two endothermic phase transitions in associated with the two main thermo-degradations of the resulting PUE nanocomposites. Moreover, DMA technique exhibited an appreciable increase in the T_g values due to a strong interaction between PTMG-modified MWCNT and PTMG-based PUE matrix.

INTRODUCTION

Owing to their widespread applications in many rapidly developing fields, MWCNT reinforced polymer-matrix composites have attracted much attention in worldwide [1–3]. To attain homogeneous and nano-dimensional dispersion of this reinforcing filler into polymer matrix, the MWCNT surface, namely the interface between the MWCNT and surrounding polymer matrix should be especially considered. To enhance MWCNT-polymer interaction, surface modification of carbon nanotubes by a variety of organic modifiers has been documented [4–10]. Although some attention is being focused on the functionalization of these inherently hard nanotubes by polyethylene glycol (PEG) [11–13] poly(tetramethylene glycol) (PTMG), which seems to be another good candidate for soft functionalization of MWCNT surface has not been reported so far.

On the other hand, among various kinds of commercially important polymers, a polyurethane elastomer (PUE) has a great potential as an appropriate matrix for MWCNT filler. Hard-soft segmented PUE materials obtained from polyether soft segments have exceptional position in polyurethane industries. Polyethylene glycol (PEG) and poly(tetramethylene glycol) (PTMG) are among the most commonly used polyethers in the preparation of PUE materials [14–17]. In addition, aliphatic and cycloaliphatic diisocyanates such as isophorone diisocyanate (IPDI) and methylenebis(cyclohexyl isocyanate) (HMDI) have been extensively used in polyurethane materials [18–22]. This kind of diisocyanates is employed often in coatings and other applications where color and transparency are important since polyurethanes made from aromatic diisocyanates tend to darken on exposure to light [23, 24].

In our previous studies regarding polyurethane-matrix nanocomposites, SiO_2 [25] and TiO_2 [26] particles were used to reinforce the thermal and mechanical properties. In the present work, however, an attempt has been made to develop a series of novel PUE-matrix composites possessing MWCNT filler in different loading contents, i.e. 0.2, 0.4, and 0.8 wt % relative to the polymer matrix. Three PTMG-based polyurethane nanocomposites encoded by PUE/MWCNT2, PUE/MWCNT4, and PUE/MWCNT8 were synthesized and characterized. Herein, a dual role has been defined for the polyether PTMG; both as the modifier of the nanotubes for preparing MWCNT-PTMG and as the initial material for the in situ preparation of the polymer matrix. Due to the structural equality between the grafted shell of the nanotubes and soft segments of the polymer matrix, it reasonably seems that the PTMG-based PUE can be uniformly loaded by PTMG-modified MWCNT. Fourier transform spectroscopy (FTIR), X-ray diffraction (XRD), scanning electron microscopy (SEM), thermogravimetric analysis (TG/DTG), differential thermal analysis (DTA), and dynamic

---

[1] The article is published in the original.

mechanical analysis (DMA) are used to characterize the resulting PUE/MWCNT nanocomposites.

EXPERIMENTAL

Materials

Methylenebis(cyclohexyl isocyanate) (HMDI, 90%) as mixture of isomers was supplied from Alfa Aesar, and used as received. Hydroxyl telechelic PTMG (HO-PTMG-OH) from Merck chemical Co. was azeotropically dried by toluene prior to use. Multi-walled carbon nanotubes (MWCNT) with outer diameter of 10−20 nm, average length of ~30 μm, and specific surface area of 200 m^2/g was purchased from Raymor Industries Inc. The nanotubes were firstly functionalized with carboxylic acid groups using nitric acid and then converted to the corresponding acid chloride (MWCNT-COCl) according to the literature [27]. Other reactants involving 1,4-butane diol (≥99%) (BD) chain extender, thionyl chloride (99%), and tri-ethylamine (TEA) were also purchased from Merck chemical Co., and used without further purification. N,N-dimethylformamide (99.5%) (DMF; Merck) was thoroughly dehydrated prior to use by calcium hydride.

Preparation of MWCNT-PTMG

The nanotubes coated by PTMG shell (MWCNT-PTMG) was prepared as follows: MWCNT-COCl (2.0 g) was homogeneously dispersed in DMF (25 mL) using an ultrasonic bath, and then poured in a 100 mL round-bottom flask. Polyether PTMG (8.0 g) and TEA (2 mL) were added to the flask, and the mixture was allowed to be stirred for 48 h at 80°C under N$_2$ flow. In order to remove the unreacted PTMG, the resulting solution was vigorously stirred in abundance of DMF solvent at room temperature for an additional 24 h. In this condition, the product (MWCNT-PTMG) was thoroughly purified, and then filtered under reduced pressure to give black solids of MWCNT-PTMG (2.66 g).

Synthesis of PUE-Matrix Nanocomposites

Into a three-necked round-bottom flask equipped with a mechanical stirrer and containing CaH$_2$-dried DMF (25 mL), diisocyanate HMDI (1.574 g, 6 mmol) was added in one portion and then fully dissolved under nitrogen atmosphere. Next, the reaction flask was charged with polyether PTMG (3.000 g, 3 mmol), and the mixture was stirred for 2.5 h at 90°C. The chain extender BD (0.27 mL, 3 mmol) was added to the resulting isocyanate-terminated prepolyurethane, and the flask ingredients was allowed to be mechanically stirred for additional 10 min. The mixture was then transferred to an appropriate glass Petri dish, and cooled to room temperature. To prepare PTMG-

based PUE nanocomposites, MWCNT-PTMG filler, was firstly homogenized in DMF (5 mL) via ultra-sonic agitation, and then slowly added to the hot vis-cose solution of the polymer. Three contents of the filler were separately used: 0.010 g (0.2 wt %), 0.019 g (0.4 wt %), and 0.039 g (0.8 wt %). Each of the films obtained were thoroughly dried in vacuum oven at 70°C to reach a fixed weight.

Characterization Methods

Fourier transform infrared spectra (FTIR) of the samples were recorded on a PERKIN ELMER RX I FTIR spectrophotometer. The spectra of the solids were obtained using KBr pellets. MIRA3 LM TES-CAN FE Scanning Electron Microscope was used for FE-SEM analysis. Prior to the capturing, the samples as $5 \times 5 \times 1$ mm^3 strips were attached to double-sided carbon tape and coated with 100 nm gold using a DC sputtering coater. X-ray diffraction (XRD) patterns were conducted at room temperature on a Bruker-D8 Advance X-ray diffractometer with Ni-filtered CuK_α radiation (30 kV, 25 mA), and λ = 1.5406 Å in the angular range of 2θ = 10°−80°. Thermogravimetric analysis (TG/DTG) and differential thermal analysis (DTA) were performed on a Simultaneous Thermal Analyzer STA 503 under argon atmosphere at a heat-ing rate of 15 grad/min in the temperature range of 25−700°C with aluminum oxide as a reference. Dynamic mechanical analysis (DMA) were measured by using a TT DMA Triton Technology, and the tests were conducted under nitrogen blanket by quenching the samples from −100 to +60°C and thereafter heating them under a frequency of 1 Hz at a rate of 3 grad/min.

RESULTS AND DISCUSSION

Synthesis Process

As Scheme 1a shows, flexible chains of polyether PTMG were covalently grafted with acylated nano-tubes (MWCNT-COCl) via formation of ester link-ages. Thus, the inherently hard nanotubes were coated by a soft organic layer composed of an HO-capped polyether. This PTMG-modified MWCNT was then loaded into a non-aromatic PUE with different load-ing contents, i.e. 0.2, 0.4, and 0.8% (by weight) relative to the matrix. The PUE matrix itself was in situ syn-thesized from PTMG polyether-polyol, HMDI diiso-cyanate, and BD chain extender (Scheme 1b). The organic layer of MWCNT is structurally equal with the soft segments of the surrounding polyurethane, which this makes the nanotubes more compatible with the matrix. The unreacted hydroxyl groups of the grafted PTMG chains allow the MWCNT-PTMG particles to be covalently linked to the macromolecules of the PUE matrix via urethane linkages (Scheme 1c), sche-matically shown with two circles). This can cause the dispersed nanotubes remain immobilized during the service life of the nanocomposite.
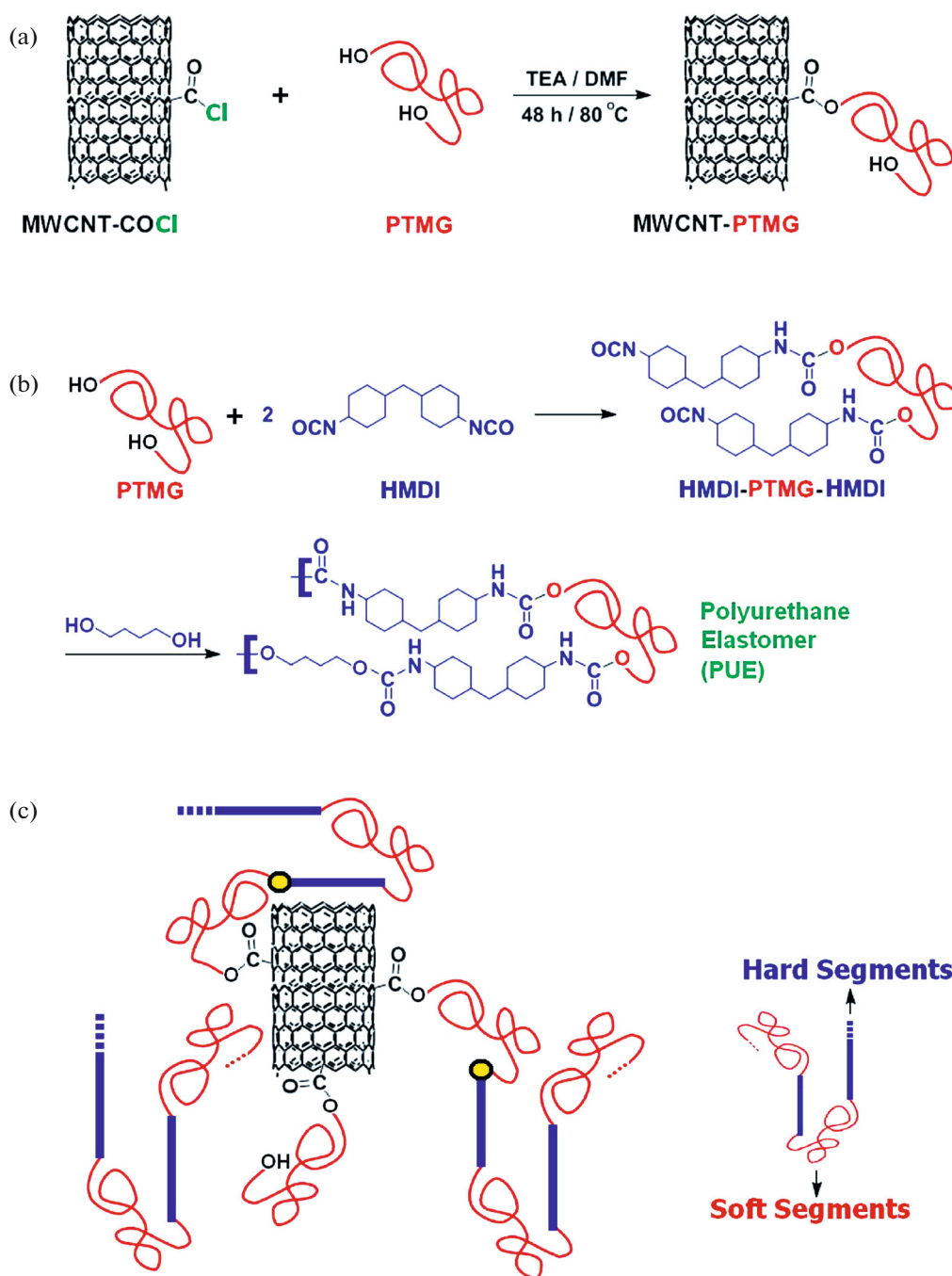
Scheme 1. (Color online).

Figure 1 shows the FTIR spectra of the PTMG-coated nanotubes (MWCNT-PTMG) and the resulting PUE/MWCNT nanocomposites. The spectra of pristine MWCNT and neat PUE are also shown for comparison purpose. According to the two upper spectra, the characteristic peaks of the PTMG modifier are also detectable in the spectrum of MWCNT-PTMG, which this indicates that covalent modification of the nanotubes by polyether PTMG has been successfully occurred. Moreover, the spectra of the

PUE-matrix nanocomposites are in agreement with those of reported in the literature [28]. As expected, the general pattern of these spectra could not be affected by the low content of the loaded PTMG-modified MWCNT. On the other hand, the mean diameter of the nanotubes increased up to 3.4 nm after covalent interaction with PTMG organic moieties. This was proved by FE-SEM images of MWCNT-PTMG particles when compared with those of pristine nanotubes. Thus, the thickness of the polyether
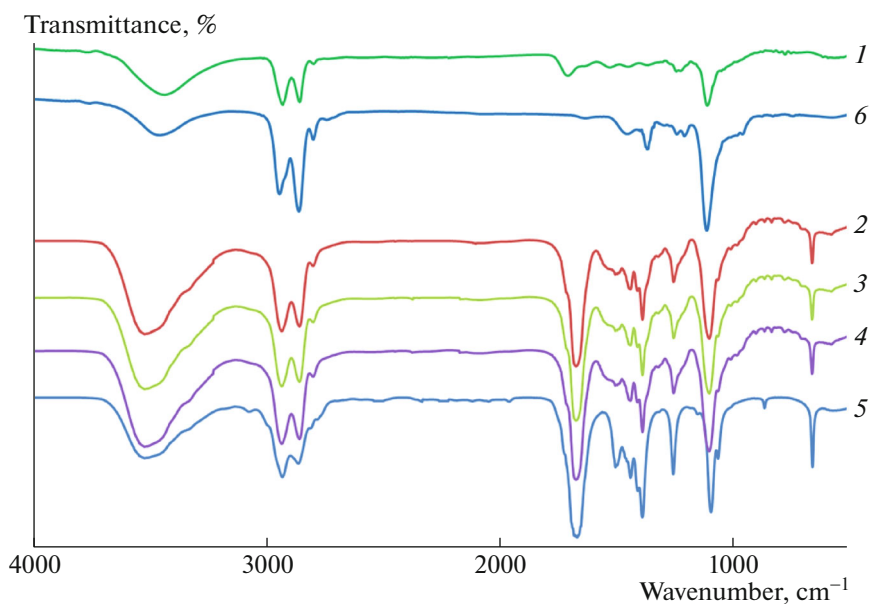
Fig. 1. (Color online) FTIR spectra of (*1*) MWCNT-PTMG, (*2*) PUE/MWCNT2, (*3*) PUE/MWCNT4, and (*4*) PUE/MWCNT8 compared with (*5*) MWCNT and (*6*) PUE/MWCNT0 references.

layer on the nanotube's wall is equal to ~1.7 nm. Figure 2 displays the micrographs of pristine MWCNT (Figs. 2a, 2b), PTMG-modified MWCNT (Figs. 2c, 2d), and PUE/MWCNT8 nanocomposite (Figs. 2e, 2f) with two magnifications. As the images show, the presence of MWCNT-PTMG particles into PUE matrix is clearly observable. No agglomeration in the modified nanotubes occurred during the polymerization reaction course. Moreover, enhancement in the mean diameter of the nanotubes can be specially observed when they are incorporated into the elastomer matrix.

Figure 3 exhibits X-ray patterns of MWCNT-PTMG particles and one of the resulting nanocomposites, PUE/MWCNT8, in comparison with the patterns of the references including the unmodified nanotubes and the neat PUE. The diffractogram of MWCNT-PTMG has an additional short peak appeared at about 20° compared to that of the unmodified nanotubes. In spite of the low content of the MWCNT-PTMG filler in the composition of the PUE-matrix nanocomposites, the two characteristic peaks of MWCNT at $2\theta = 26°$ and $43°$ are still somewhat observable in the XRD pattern of the PUE/MWCNT8.

Thermogravimetric Analysis

Figure 4 exhibits TG/DTG thermograms of PTMG-modified MWCNT and the corresponding PUE-matrix nanocomposites together with unmodified MWCNT and neat PUE. The maximum thermal destruction of MWCNT-PTMG particles occurred at the range of 250−290°C. This destruction is ascribed mainly with cleavage of the ester linkages and conse-

quently removal of the polyether PTMG. Moreover, the residue weight of MWCNT-PTMG particles at 700°C was found to be 76%. This indicates that about 24% of the weight of the modified nanotubes is formed by the grafted PTMG shell. Based on the overweight of the pristine MWCNT after the modification reaction (0.66 g), the above-mentioned percent is expectable. As expected, like other polyurethane materials, thermal degradation of these polyurethanes occurred in two stages, ranging from 340−400 and 420−480°C. The first stage is mainly related to the degradation of the hard segments and the second stage is associated with the degradation of the soft segments [29]. As the thermograms show, due to the addition of MWCNT-PTMG particles to the polyurethane matrix, a thermo-stability, but not so much, could be observed throughout the temperatures. Some data resulted from TG/DTG analysis such as onset temperature of degradation (T_{onset}), the temperatures of 5 and 10% decompositions ($T_{d5\%}$ and $T_{d10\%}$), and two temperatures associated with the two maximum destructions (T_{max1} and T_{max2}) are also tabulated in Table 1.

Differential Thermal Analysis

Figure 5 shows DTA profiles of the nanocomposites obtained at elevated temperatures. Two major phase transitions, both caused by endothermic processes, could be observed. These transitions occurred at thermal regions around 350 and 450°C, which are fully congruous with the two main thermo-degradations of the nanocomposites. Hence, the peaks appeared in the DTA thermograms are associated with the decomposition of soft and hard segments of the
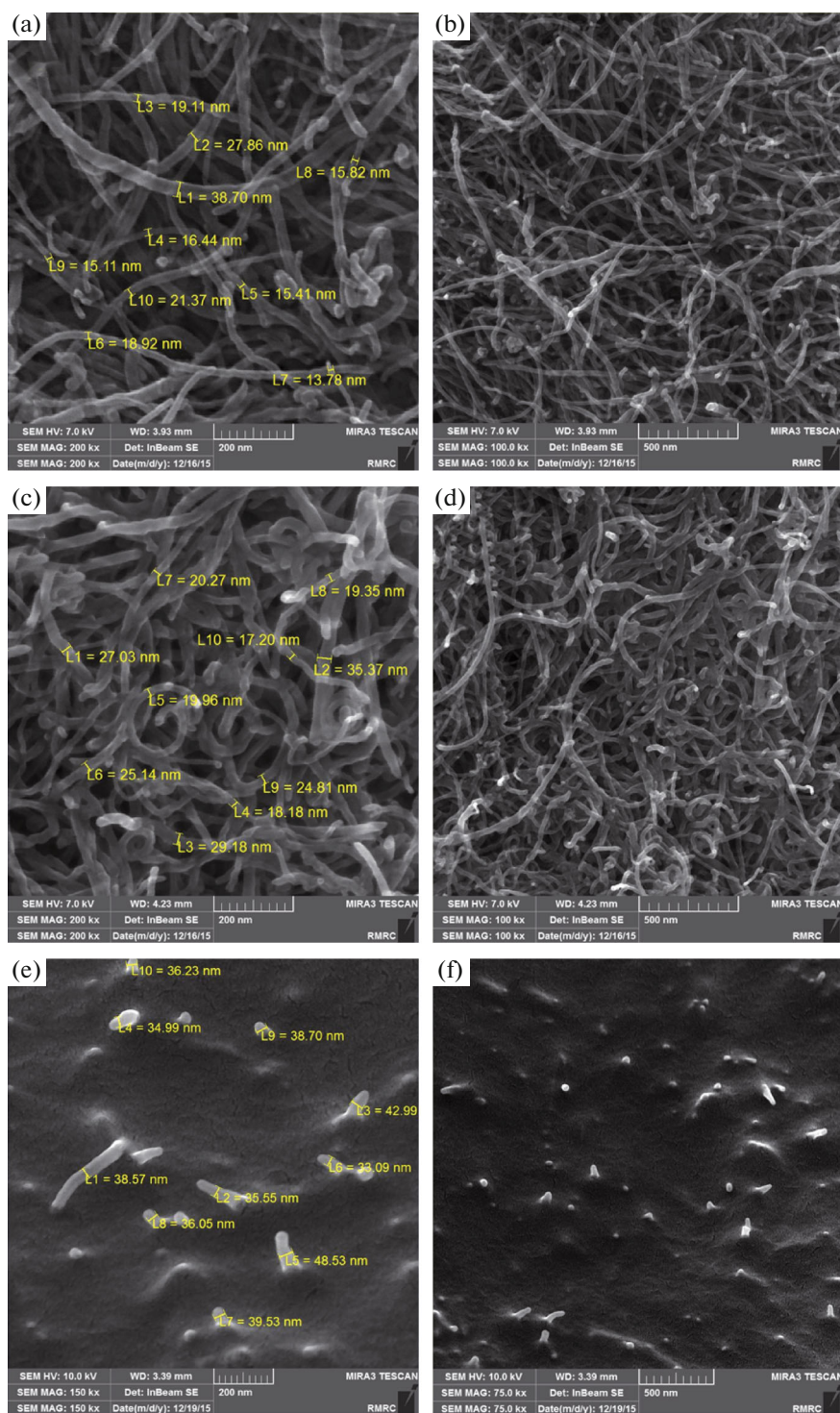
Fig. 2. (Color online) (a, b) FE-SEM images of pristine MWCNT, (c, d) MWCNT-PTMG, and (e, f) PUE/MWCNT8 nano-composite.

polyurethane chains. Although if atmosphere is switched from inert to air/oxygen sometimes decom-position becomes exothermic, the phenomenon of decomposition should be usually endothermic as heat is required to break chemical bonds in the compound undergoing decomposition.

Dynamic Mechanical Analysis

The resulting PUE/MWCNT nanocomposites were examined by DMA technique. Figure 6 displays tan δ—temperature plots of the nanocomposites obtained in comparison with the neat PUE. According
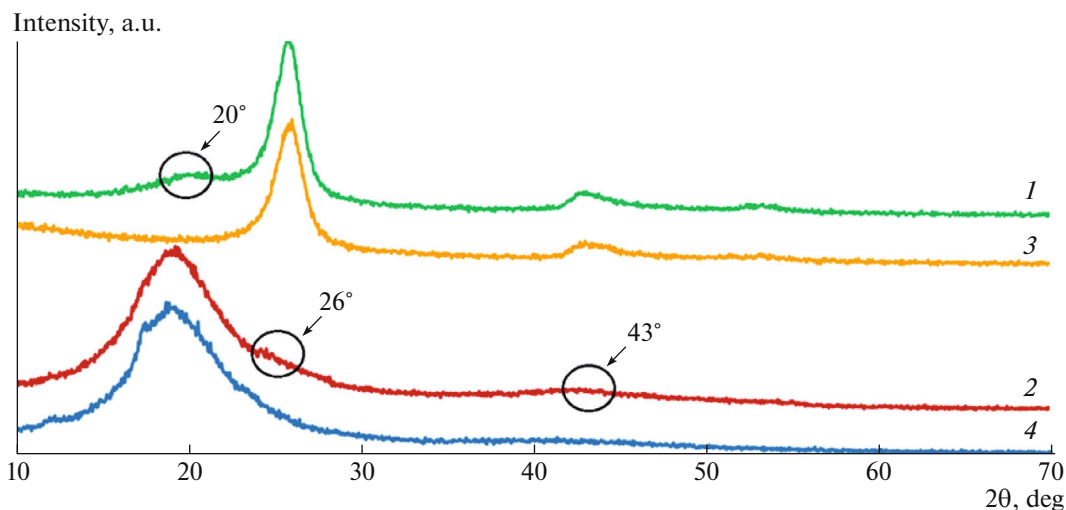
Fig. 3. (Color online) X-ray diffractograms of (*1*) MWCNT-PTMG and (*2*) PUE/MWCNT8 compared with the diffractograms of (*3*) MWCNT and (*4*) PUE/MWCNT0 references, respectively.

to the peaks observed, T_g values of PUE/MWCNT2, PUE/MWCNT4, and PUE/MWCNT8 were found to be −10, −4, and −2°C, respectively. Based on the results obtained, a significant difference, up to 10°C, can be observed, when the T_g values of PUE/MWCNT8 and the neat PUE are compared with each other. Also, the T_g value increases with increasing the loading content of MWCNT-PTMG particles. This indicates that the segmental motions of the macromolecular chains are relatively restricted by the addition of the nanofiller to the PUE matrix. An enhanced interaction could be established between the components of the composites, which led to a decrease in chain mobility. Homogeneous dispersion of MWCNT-PTMG particles within the PUE matrix can also be deduced here because it has been demonstrated that heterogeneous and bulk dispersion of fillers into a polymer matrix decreases intermolecular interactions. Contrary to the homogeneous dispersions, this unfavorable dispersion lead to an increase in the chain mobility of the macromolecules; consequently, a decrease in the T_g value of the polymer is observed [30, 31]. The homogeneous dispersion of MWCNT-PTMG particles arises from the strong interaction between the nanofiller and PTMG-based PUE. All of these originate from a structural equality; the modified nanotubes and the PUE matrix both are formed from PTMG. Moreover, the storage moduli of PUE/MWCNT2, PUE/MWCNT4 and PUE/MWCNT8 nanocomposites at some temperatures around their glass transition temperatures (T_g) were determined and compared with those of PUE/MWCNT0 neat polymer. The results (Table 2) clearly show that the modulus of the resultant elastomers increases due to the incorporation of MWCNT-PTMG particles into the polymer matrices.

Table 1. Some TG/DTG data of MWCNT-PTMG nanoparticles, and PUE/MWCNT2, PUE/MWCNT4 and PUE/MWCNT8 nanocomposites

Entry	Code	$T_{onset}{}^a$, °C	$T_{d5\%}{}^b$, °C	$T_{d10\%}{}^c$, °C	$T_{max1}{}^d$, °C	$T_{max2}{}^e$, °C
1	MWCNT-PTMG	225	260	271	270	–
2	PUE/MWCNT2	296	331	348	385	428
3	PUE/MWCNT4	296	335	349	385	429
4	PUE/MWCNT8	306	335	349	385	429
5	PUE/MWCNT0	271	327	342	381	428

^{a} Onset temperature of decomposition.

^{b} Temperature of 5% weight loss from TG analysis.

^{c} Temperature of 10% weight loss from TG analysis.

^{d} Temperature of the first maximum decomposition from DTG analysis.

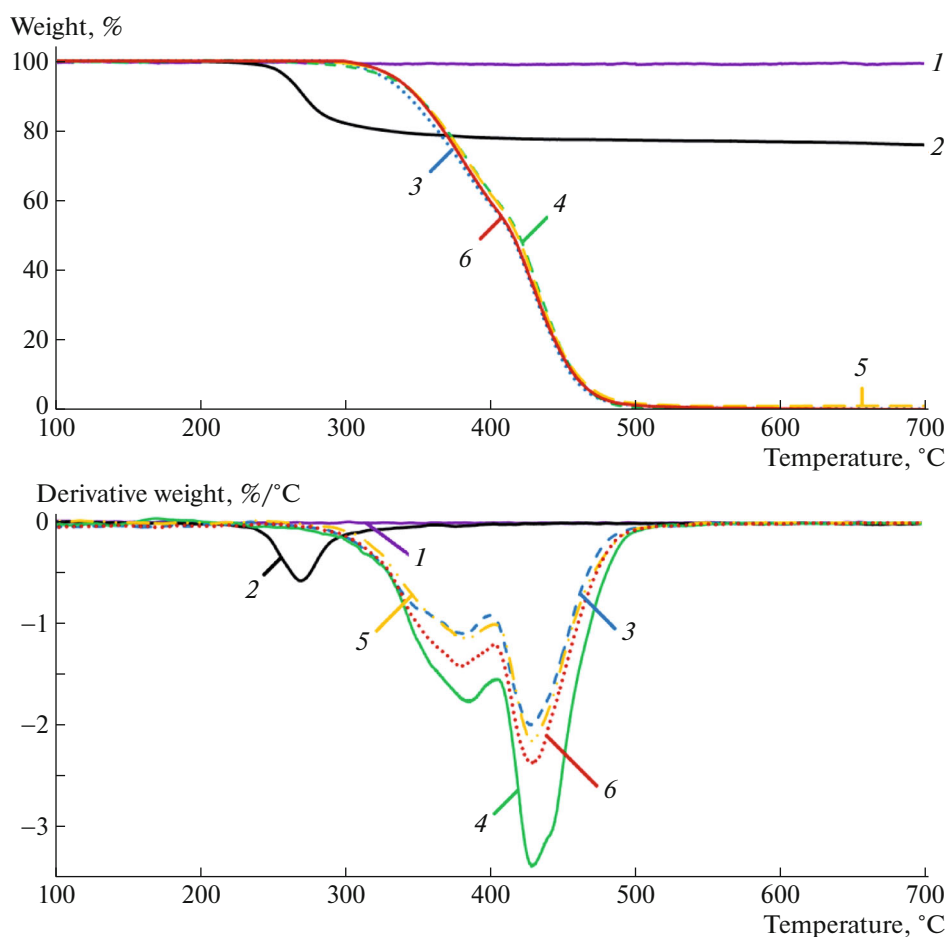^{e} Temperature of the second maximum decomposition from DTG analysis.

Fig. 4. (Color online) (a) TG and (b) DTG thermograms of (*1*) MWCNT, (*2*) MWCNT-PTMG, and the resulting PUE/MWCNT nanocomposites: (*3*) PUE/MWCNT0, (*4*) PUE/MWCNT2, (*5*) PUE/MWCNT4, (*6*) PUE/MWCNT8.

CONCLUSIONS

Preparation of polymer-matrix nanocomposites loaded by MWCNT is generally encountered with the challenge of heterogeneous dispersion of the nanotubes into the polymer matrix due to their agglomeration during loading process. In this study, it was demonstrated that if polyether PTMG is covalently grafted to MWCNT, and then these modified nanotubes are loaded into a PTMG-based PUE, an excel-lent filler-matrix interaction can be achieved. Since polyurethane elastomers of PTMG have been considered as the polymer matrix, MWCNT filler were reasonably modified by PTMG shell. In such a condition, a uniformly dispersion of MWCNT-PTMO filler into the PUE matrix could be resulted, which this itself originates from the structural similarity between PTMG-modified guest and PTMG-based PUE host. It seems that this strategy can be successfully general-

Table 2. Some storage moduli of PUE/MWCNT2, PUE/MWCNT4 and PUE/MWCNT8 nanocomposites compared to those of PUE/MWCNT0 neat polymer

Entry	Code	$E'_{-40°C}{}^{a}$, GPa	$E'_{-30°C}{}^{b}$, GPa	$E'_{-20°C}{}^{c}$, GPa	$E'_{-10°C}{}^{d}$, GPa	$E'_{0°C}{}^{e}$, GPa	$E'_{+10°C}{}^{f}$, GPa
1	PUE/MWCNT2	0.969	0.544	0.223	0.087	0.041	0.023
2	PUE/MWCNT4	1.023	0.567	0.248	0.092	0.037	0.018
3	PUE/MWCNT8	0.915	0.556	0.263	0.109	0.048	0.025
4	PUE/MWCNT0	0.837	0.412	0.170	0.070	0.034	0.020

$a–f$Storage moduli at −40, −30, −20, −10, 0, and +10°C from left to right, respectively.
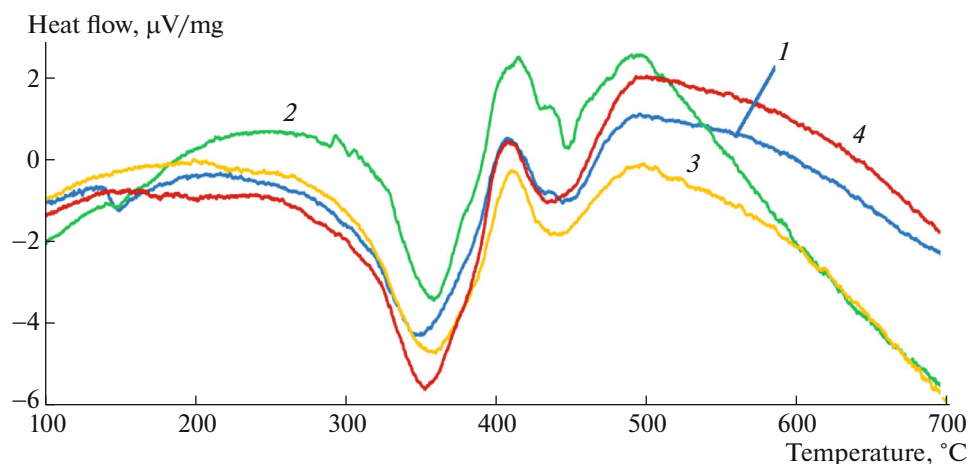
Fig. 5. (Color online) DTA profiles of (*1*) the neat PUE and the resulting PUE-matrix nanocomposites: (*2*) PUE/MWCNT2, (*3*) PUE/MWCNT4, (*4*) PUE/MWCNT8.
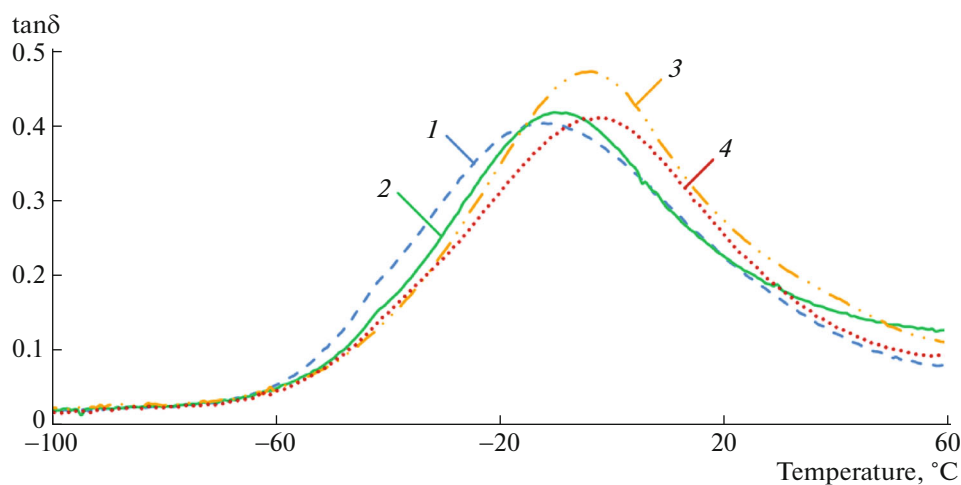

Fig. 6. (Color online) tan δ—temperature curves of (*1*) the neat PUE and the resulting PUE-matrix nanocomposites: (*2*) PUE/MWCNT2, (*3*) PUE/MWCNT4, (*4*) PUE/MWCNT8.

ized for preparing each polymer-matrix composite possessing nano-dimensional fillers.

REFERENCES

1. B. P. Grady, *Carbon Nanotube-Polymer Composites* (John Wiley & Sons, Inc., Hoboken; New Jersey, 2011).

2. V. Georgakilas, J. A. Perman, J. Tucek, and R. Zboril, Chem. Rev. **115** (11), 4744 (2015).

3. N. G. Sahoo, S. Rana, J. W. Cho, L. Li, and S. H. Chan, Prog. Polym. Sci. **35** (7), 837 (2010).

4. N. Karousis, N. Tagmatarchis, and D. Tasis, Chem. Rev. **110** (9), 5366 (2010).

5. D. Vairavapandian, P. Vichchulada, and M. D. Lay, Anal. Chim. Acta **626** (2), 119 (2008).

6. S. W. Kim, T. Kim, Y. S. Kim, H. S. Choi, H. J. Lim, S. J. Yang, and C. R. Park, Carbon **50** (1), 3 (2012).

7. M. F. L. De Volder, S. H. Tawfick, R. H. Baughman, and A. J. Hart, Science **339** (6119), 535 (2013).

8. F. Zhou, S. Wu, S. Song, W. R. Chen, D. E. Resasco, and D. Xing, Biomaterials **33** (11), 3235 (2012).

9. C. Gao, Z. Guo, J. H. Liu, J.-H. Liu, and X.-J. Huang, Nanoscale **4**, 1948 (2012).

10. S. Mallakpour and A. Zadehnazari, J. Thermoplast. Compos. Mater. **28** (12), 1644 (2015).

11. M. Bottini, N. Rosato, and N. Bottini, Biomacromolecules **12** (10), 3381 (2011).

12. C. K. Jang, J. H. Park, and J. Y. Jaung, Mater. Res. Bull. **47** (10), 2767 (2012).

13. C. Sacchetti, K. Motamedchaboki, A. Magrini, G. Palmieri, M. Mattei, S. Bernardini, N. Rosato, N. Bottini, and M. Bottini, ACS Nano **7** (3), 1974 (2013).

14. D. Fragiadakis and J. Runt, Macromolecules **46** (10), 4184 (2013).

15. F. Rafiemanzelat, A. Fathollahi-zonouz, and G. Emtiazi, Polym. Degrad. Stab. **97** (1), 72 (2012).

16. Q. Tang, Q. Ai, R. Yang, and J. He, Polym. Sci., Ser. A **56** (4), 441 (2014).

17. H.-J. Kim, M.-S. Kang, J. C. Knowles, and M.-S. Gong, J. Biomater. Appl. **29** (3), 454 (2014).

18. S. M. Hasan, J. E. Raymond, T. S. Wilson, B. K. Keller, and D. J. Maitland, Macromol. Chem. Phys. **215** (24), 2420 (2014).

19. D. P. Suhas, H. M. Jeong, T. M. Aminabhavi, and A. V. Raghu, Polym. Eng. Sci. **54** (1), 24 (2014).

20. B. Ates, S. Koytepe, M. G. Karaaslan, S. Balcioglu, and S. Gulgen, Int. J. Adhes. Adhes. **49**, 90 (2014).

21. A. Domanska and A. Boczkowska, Polym. Degrad. Stab. **108**, 175 (2014).

22. H. Janik and M. Marzec, Mater. Sci. Eng., C **48**, 586 (2015).

23. B. P. Thapliyal and R. Chandra, Prog. Polym. Sci. **15** (5), 735 (1990).

24. C. R. Newman and D. Forciniti, Ind. Eng. Chem. Res. **40** (15), 3346 (2001).

25. H. Behniafar and S. Azadeh, Int. J. Polym. Mater. **64** (1), 1 (2014).

26. H. Behniafar, M. Alimohammadi, and K. Malekshahinezhad, Prog. Org. Coat. **88**, 150 (2015).

27. R. Gao, S. M. Ramirez, D. L. Inglefield, R. J. Bodnar, and T. E. Long, Carbon **54**, 133 (2013).

28. K. Nakayama, T. Ino, and I. Matsubara, J. Macromol. Sci., Part A: Pure Appl. Chem. **3** (5), 1005 (1969).

29. Z. S. Petrovic, Z. Zavargo, J. H. Flynn, and W. J. Macknight, J. Appl. Polym. Sci. **51** (6), 1087 (1994).

30. D. Carponcin, E. Dantras, J. Dandurand, G. Aridon, F. Levallois, L. Cadiergues, and C. Lacabanne, J. Non-Cryst. Solids **392**, 19 (2014).

31. J. R. Potts, D. R. Dreyer, C. W. Bielawski, and R. S. Ruoff, Polymer **52** (1), 5 (2011).